High-temperature electron-hole liquid and dynamics of Fermi excitons in a $In_{0.65}Al_{0.35}As/Al_{0.4}Ga_{0.6}As$ quantum dot array

C. R. Ding and H. Z. Wang*
State Key Laboratory of Optoelectronic Materials and Technologies, Zhongshan (Sun Yat-Sen) University, Guangzhou 510275, China

B. Xu
Key Laboratory of Semiconductor Materials Science, Institute of Semiconductors, Chinese Academy of Sciences, Beijing 100083, China
(Received 9 August 2004; revised manuscript received 20 October 2004; published 4 February 2005)

State-filling effects of the exciton in a $In_{0.65}Al_{0.35}As/Al_{0.4}Ga_{0.6}As$ quantum dot array are observed by quantum dot array photoluminescence at a sample temperature of 77 K. The exciton emission at low excitation density is dominated by the radiative recombination of the states in the *s* shell and at high excitation density the emission mainly results from the radiative recombination of the exciton state in the *p* shell. The spectral interval between the states in the *s* and *p* shells is about 30–40 meV. The time resolved photoluminescence shows that the decay time of exciton states in the *p* shell is longer than that of exciton states in the *s* shell, and the emission intensity of the exciton state in the *p* shell is superlinearly dependent on excitation density. Furthermore, electron-hole liquid in the quantum dot array is observed at 77 K, which is a much higher temperature than that in bulk. The emission peak of the recombination of electron-hole liquid has an about 200 meV redshift from the exciton fluorescence. Two excitation density-dependent emission peaks at 1.56 and 1.59 eV are observed, respectively, which result from quantum confinement effects in QDs. The emission intensity of electron-hole liquid is directly proportional to the cubic of excitation densities and its decay time decreases significantly at the high excitation density.

DOI: 10.1103/PhysRevB.71.085304 PACS number(s): 78.55.Cr, 71.35.Ee, 78.47.+p

I. INTRODUCTION

Semiconductor self-assembled quantum dot (QD) heterostructrues, with the carriers being confined to an essentially zero-dimensional structure, make them an excellent systems for basic physics studies, as well as technological applications. Optical interactions with these systems are of critical importance because optical spectroscopy provides insight into their electron structure and dynamics. The theoretical study[1] describes that the electron and hole occupy the confined electronic and hole energy and indicate the state-filling effect in characteristic numbers according to the Pauli exclusion principle, and experimental studies[2–5] give evidences of this state-filling effect of excitons at the QD energy level. Among them, in an isolated single $In_xAl_{1-x}As/Al_yGa_{1-y}As$ QD, state-filling effects of excitons are also observed at 1.2 K. Nevertheless, the transition dynamics of the exciton distributing on different shells of a QD array has not been studied.

In this paper, state filling effects of Fermi exciton and the dynamics of exciton states in the *s* and *p* shells of an ensemble of an $In_{0.65}Al_{0.35}As/Al_{0.4}Ga_{0.6}As$ quantum dot array are observed and their temporal properties are studied by time-resolved laser spectroscopy. On the other hand, at high excitation density, the photogenerated dense electron-hole liquid (EHL) of which the physical properties are similar to those of liquefied metals[6] has been an important research subject. EHL has been observed in Si,[7] GaP,[8] AlGaAs,[9] SiC,[10] and diamond.[11] In these indirect-gap semiconductors, the density of photogenerated carries can be varied within a wide range. The transformation from an insulator to a metallic phase is referred to as the exction Mott transition at the critical temperature (T_c), above which the exciton will be not condense to liquid. In direct-gap semiconductors CuCl (Ref. 12) and CdS,[13] the situation is more complicated because the system has more difficulties in reaching quasiequilibrium during the carrier lifetime. This is one of reasons that the T_c of EHL in direct-gap semiconductors is much lower than that of indirect-gap semiconductors, such as the highest T_c of direct-gap semiconductors is 55 K for CdS, while that of indirect-gap semiconductor diamond is 167 K. In the past, the study of EHL is focused on bulk material, and the characteristics of EHL in the QD system has not been revealed until now, while the QD array system is interesting from the point of view of basic physics for studying EHL.

In this work, our experimental results indicate that the electron-hole liquid in a quantum dot array can be formed at much higher temperature than that in bulk, and some quantum confinement phenomena in QD are observed.

II. EXPERIMENTS

The self-assembled $In_{0.65}Al_{0.35}As/Al_{0.4}Ga_{0.6}As$ QD array is grown by molecular beam epitaxy on semi-insulating (1 0 0)-oriented GaAs substrate with a 500-nm N^+-GaAs buffer layer. The self-assembled QDs are obtained using the spontaneous island formation in the initial stages of the Stranski-Krastanow growth mode during the epitaxy of highly strained $In_{0.65}Al_{0.35}As/Al_{0.4}Ga_{0.6}As$ layer. It is an undoped heterostructure with six layers of $In_{0.65}Al_{0.35}As$ (usually five-monolayer overage) quantum dots. A 10-nm layer of $Al_{0.4}Ga_{0.6}As$ barrier layer separates each dot layer. These six layers are sandwiched between two 200-nm-thick AlGaAs waveguide layers and two 1500-nm N-AlGaAs carrier con-

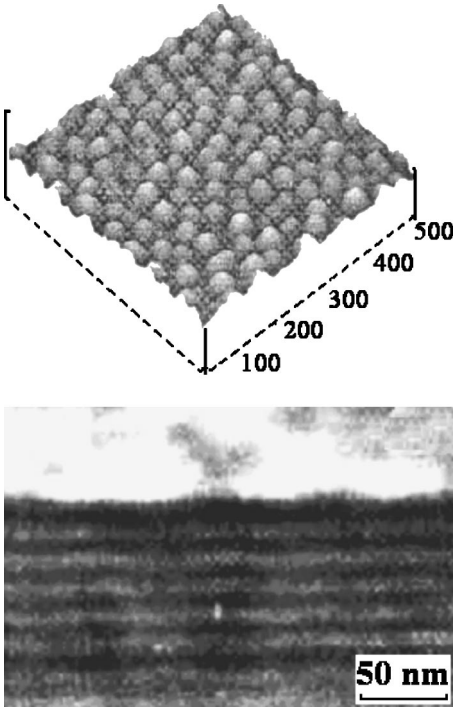

FIG. 1. (a) Atomic force micrograph image of an $In_{0.65}Al_{0.35}As/Al_{0.4}Ga_{0.6}As$ quantum dot array. (b) Cross-sectional transmission electron microscopy image of the active region of an $In_{0.65}Al_{0.35}As/Al_{0.4}Ga_{0.6}As$ quantum-dot array.

finement layers. A 300-nm P^+-GaAs cladding layer acts as an up-contacting layer that is subsequently removed through etching to enable optical measurements. The $In_{0.65}Al_{0.35}As$ dots are grown at 530 °C while the rest of the sample is grown at 600 °C. Six dot layers are grown without generating additional defects to improve the dot uniformity and to increase the photoluminescence signal levels. The lens-shaped $In_{0.65}Al_{0.35}As$ quantum dot is a part of a sphere with a fixed height of 3.4 nm and base diameters of 38 nm. Atomic force microscopy scans reveal a dot density of about 5×10^{10} cm^{-2} per layer. A more detailed description of the fabrication of $In_{0.65}Al_{0.35}As/Al_{0.4}Ga_{0.6}As$ self-assembled quantum dots can be found in Ref. 14. Figure 1(a) is an atomic force micrographs image of the surface of one-layer $In_{0.65}Al_{0.35}As/Al_{0.4}Ga_{0.6}As$ QD, and Fig. 1(b) is a cross-sectional transmission electron microscopy image illustrating the vertically aligned six-layer $In_{0.65}Al_{0.35}As/Al_{0.4}Ga_{0.6}$ QD array. The optical measurement is performed with a frequency double mode-locked Nd:YAG laser (Spectra Physics, Model 3000) operating with a repetition rate of 82 MHz and 80 ps pulse duration as an excitation source. The excitation laser is focused through a lens of focal length $f=55$ mm to a spot radius of about 116 μm. All measurements presented in this paper are performed at a sample temperature of 77 K in a liquid nitrogen cryostat. The emission is detected by a synchronously streak camera (Hamamatsu Model C1587, time resolution of 10 ps) connected to a polychromator. The photoluminescence signal is collected in a backscattered geometry.

III. RESULTS AND DISCUSSION

A. State filling of Fermi excitons and its transient behavior

Photoluminescence experiments are performed at various excitation densities. Figure 2(a) shows the state-filling spectroscopy of exciton and multiexciton shows state-filling spectroscopy of exciton and multiexciton with the excitation densities ranging between 0.29 and 1420 W/cm^2. At an excitation density not higher than 1.24 W/cm^2, only the emission of state in the unsaturated *s* shell (at 1.776 eV) is observed. As the excitation density increaeses to 2.43 W/cm^2, the emission of the saturated *s* shell has a redshift. At an excitation density of 59.6 W/cm^2, the emission is dominated by states in the *p* shell, which has a 30–40 meV blueshift than that of in the *s* shell. Further increasing the excitation density (such as higher than 355 W/cm^2), the emission has a

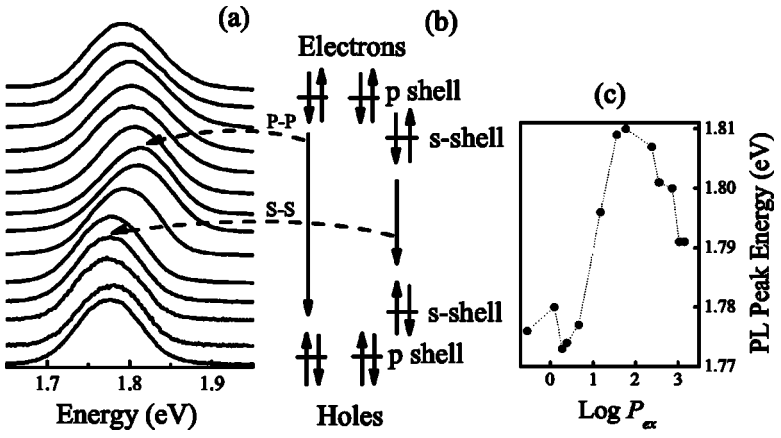

FIG. 2. Photoluminescence spectra of exciton in an $In_{0.65}Al_{0.35}As/Al_{0.4}Ga_{0.6}As$ quantum dot array for different excitation density at 77 K. The spectra are normalized and vertically offset for clarity. (a) State-filling spectra on quantum dots. The spectra from the lowest to the uppermost are recorded, respectively, at excitation densities of $P_{ex}=0.29$, 1.24, 1.92, 2.43, 4.68, 15.2, 36.5, 59.6, 243, 355, 365, 737, 1065, and 1420 W/cm^2. (b) A sketch of quantum dot energy levels distributing exciton and multiexcitons. Spin orientations are sketched with arrows. (c) Spectral peak energy of the exciton emission (●) as a function of the logarithm of the excitation density ($\ln P_{ex}$). The dot line is a guide.

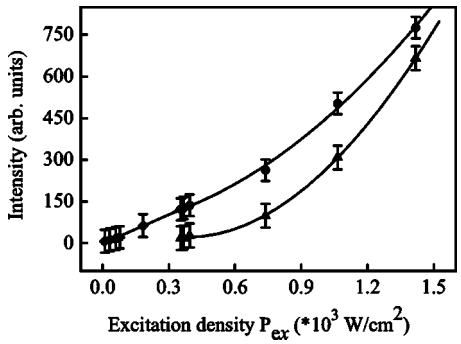

FIG. 3. The excitation density dependence of the integrated luminescence of exciton (●) and EHL (▲) in an $In_{0.65}Al_{0.35}As/Al_{0.4}Ga_{0.6}As$ quantum dot array. The solid line is guidance of nonlinear dependence.

obvious redshift than that at 59.6 W/cm^2, which means that multiexciton states in the *p* shell dominate the emission. Figure 2(b) shows a sketch of the radiative transition of exciton and multiexcitons distributing on fully or partially filled shells of QD arrays. The shell in QD arrays is populated with an increasing number of carriers according to Fermi statistics principle. Figure 2(c) shows the peak energy of the recombination of exciton in QD arrays as a function of the excitation densities. These states in the *s* and *p* shells are degenerate except for a slight difference due to Coulomb exchange and correlation interactions among carriers.[15]

The solid cycle curve in Fig. 3 shows the time-integrated emission intensity of the exciton as a function of the excitation density. As the excitation density is lower than 59.6 W/cm^2, only the recombination of the state in the *s* shell and the recombination of a single exciton state in the *p* shell occurs (see Fig. 2). The emission intensity is linearly proportion to the excitation density. As the excitation density is higher than 355 W/cm^2, the recombination of multiexciton states in the *p* shell (see Fig. 2) is dominated; the relationship between the emission intensity and the excitation density can be fitted by a function of $I=132P_{ex}^2-10.5P_{ex}+80.9$, indicated by a solid line in Fig. 3.

The decay times of single exciton states in the *s* and *p* shells as well as multiexciton states in the *p* shell are shown in Fig. 4. The decay time of single exciton states in the *s* shell at an excitation density of 0.29 W/cm^2 is 395 ps (solid line). The decay time of single exciton state in the *p* shell at excitation density of 59.6 W/cm^2 is 399 ps (dash line). The decay time of multiexciton states in the *p* shell at excitation density of 1420 W/cm^2 is 428 ps as shown in (dot line).

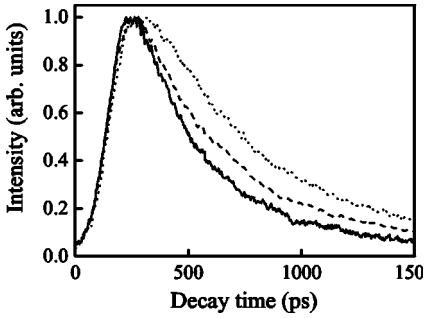

FIG. 4. Decay times of a single exciton state in the *s* shell (solid line) and in the *p* shell (dash line), and decay time of multiexciton states in the *p* shell (dot line) as well. The spectra are normalized for clarity.

The phenomena above can be discussed as follows. First, the concept of the state-filling effect means that the shells are populated according to Pauli exclusion principle. The *s* shell is twofold spin degenerate, and can be occupied by not more than two excitons. The emission peak of the state in the saturated *s* shell has a slight redshift, which originates from the electron-electron and hole-hole interactions as well as correlation effects.[15] The *p* shell can hold a maximum of four electron-hole pairs. The recombination of the states in the *s* and *p* shells indicates a remarkable dependence on the number of exciton, which is explained by the fundamental principle of hidden symmetries associated with this degeneracy as a rule determining the electronic structure of electron-hole complexes in quantum dots.[1,3,16]

Secondly, inhomogeneous broadening of QD results in that the radiative emission of states in the *s* and *p* shells cannot be discerned as that of states in a single QD. However, the vertical coupling of multilayered QD arrays is beneficial to sharpen the emission bend,[3,17,18] which makes state-filling effects can be directly observed in QD arrays.

Thirdly, that the decay time of multiexciton states in the *p* shell is longer than that of single exciton can be explained as follows: the electron distributing in larger region for saturated *p* shell, which decreases probability of recombination of excitons; and Pauli blocking more strongly prevents the state in the *p* shell from rapidly relaxing as comparison to the state in the *s* shell of QD arrays.[19]

B. Electron-hole liquid with high temperature in the quantum dot array

In the photoluminescent experiment, a new emission band at 1.56 eV is observed in $In_{0.65}Al_{0.35}As/Al_{0.4}Ga_{0.6}As$ QD arrays at an excitation density higher than 243 W/cm^2. Figure 5(a) shows the time-resolved photoluminescent spectrum of QD arrays at the excitation density of 1065 W/cm^2, in which the band around 1.79 eV is the exciton emission band, and the emission around 1.59 eV is the emission band of EHL in QD arrays. The phenomena and their properties will be described in detail as follows.

First, as shown in Fig. 5(a), the emission band of EHL has a redshift of 200 meV from the excitom emission band.

Second, Figure 5(b) shows the spectral profiles of EHL band at the time of 109, 217, 327, 826, and 954 ps after excitation and at the excitation density of 1065 W/cm^2. While Fig. 5(c) shows the spectral profiles of EHL band at excitation densities of 243, 355, 365, 737, 1605, and 1420 W/cm^2, respectively. Figures 5(b) and 5(c) reveal a new phenomenon: there are two states in EHL in QD, one appears at high excitation density (such as 737, 1065, and 1420 W/cm^2, or at the first half of decay curve of high excitation density). The other appears at low excitation density or at the tail of decay process. Both spectral profiles do not change within rather wide range of the excitation density. It means that quantized states exist in EHL.

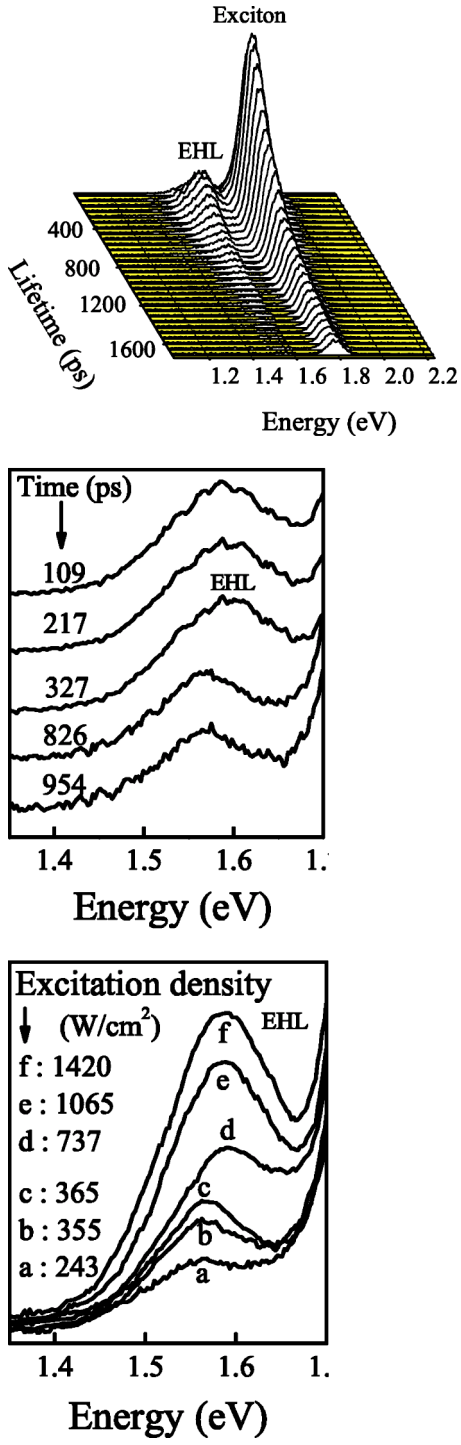

FIG. 5. (a) Time-resolved photoluminescence spectrum of $In_{0.65}Al_{0.35}As/Al_{0.4}Ga_{0.6}As$ quantum dot array at the excitation density of 1065 W/cm^2 and 77 K. Exciton: the exciton emission band; EHL: electron-hole liquid emission band with the peak energy of 1.59 eV. (b) The spectra show time-resolved luminescence spectra of EHL at times of 109, 217, 327, 826, 954 ps after excitation. The spectra are normalized to the emission intensity of EHL and are offset for clarity. (c) The spectra are illustrated for different excitation densities of (a) 243, (b) 355, (c) 365, (d) 737, (e) 1065, and (f) 1420 W/cm^2. The spectra are normalized to the emission intensity of exciton.

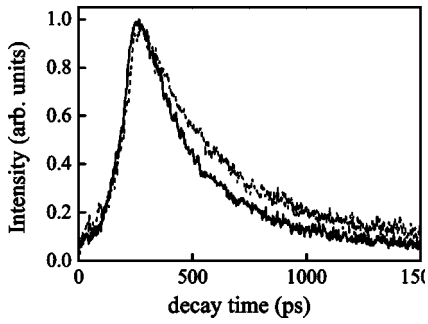

FIG. 6. Decay times of EHL bands at lower excitation density of 355 W/cm^2 (dash line) and at a higher excitation density of 1120 W/cm^2 (solid line). The spectra are normalized for clarity.

Third, the dash curve in Fig. 6 demonstrates the decay time of EHL band at lower excitation density of 355 W/cm^2, the decay time is about 360 ps. The solid curve in Fig. 6 shows the decay time of EHL band at higher excitation density of 1120 W/cm^2, which is obviously shorter than that at the lower excitation density.

Fourth, the solid triangle curve in Fig. 3 shows the relationship of time-integrated emission intensity of the EHL and the excitation density, which can be fitted by a function of $I=32.5P_{ex}^3+90.4P_{ex}^2-132.5P_{ex}+60.7$, where P_{ex} is the excitation density.

These phenomena about the EHL above can be discussed as follows.

First, for this sample, there is no known emission around 1.56–1.59 eV except from EHL and GaAs substrate. The emission band of GaAs substrate is at 1.493 eV,[5,20,21] and its excitation density-dependent properties (including temporal, spectral, and intensity) are entirely different from experimental results above. Therefore, the phenomenon observed in this work is EHL in QD arrays.

Secondly, the high critical temperature (T_c) can be discussed as follows. (1) The spatial confinement in QD is in favor of EHL formation. The binding energy of EHL is associated to the confinement potential and perturbed by Coulomb-exchange and -correlation interactions among carriers. As the exchange- and correlation-induced interactions among the high-density photogenerated carriers in QDs are enough to circumvent the Fermi repulsive potential due to Coulomb screening among electrons or holes and to reduce the chemical potential below the electron-hole pair energy, and electron-hole pairs become ionized, i.e., the Fermi condensate in the forms of EHL appears. (2) The discrete energy level of QD makes interactions of carriers with acoustic phonons being inhibited (phonon bottleneck). Carriers in QD usually exhibits much long dephasing time than that in the bulk,[22] which benefits the electron-hole system to reach quasiequilibrium,[12] in particular for coupled QDs.[23] (3) The decrease of the dielectric constant in QD also contributes to the formation of EHL.[11] (4) Using the modified Thomas-Fermi screening approximation, the critical density (n_{Mott}^{TF}) of the exciton Mott transition is described as[11] $n_{Mott}^{TF}=(4\alpha_B)^3=1.56\times10^{16}/\text{cm}^3$ corresponding to the excitation density of 208 W/cm^2, the critical temperature (T_c) (Ref. 7) of EHL is $T=8\pi e^2\alpha_B^2 n_{Mott}/1.19^2\varepsilon(r)k_B=106$ K, where $\alpha_B=10$ nm

(Ref. 24) is electron-hole pair Bohr radius in QD and $\varepsilon(r)$ is the dielectric constant of QD. In $In_{0.65}Al_{0.35}As/Al_{0.4}Ga_{0.6}As$ self-assembled quantum dots, exciton Bohr radius is larger than the height of QD ($r=3.4$ nm), and the strong confinement effects of QD overcome the Coulomb screening effect[25] and reduce the dielectric constant.[26,27] The size-dependent dielectric constant is given by[25,27,28] $\varepsilon(r)=1+(\varepsilon_{\text{bulk}}-1)/[1+(9.7/r)^{1.3}]=10.2$, where $\varepsilon_{\text{bulk}}=12$.[29]

Thirdly, about the new phenomenon of quantized states of EHL, it implies that at lower excitation (243–365 W/cm^2), electrons and holes has a certain density. Then, at higher excitation (737–1420 W/cm^2), if the density of electrons and holes in EHL is still same as that at lower excitation density, the volume of EHL may be larger than that of QD, which is impossible since they cannot go out from QD, therefore, the higher state of EHL appears. As high density excitation, most of decay time is dominated by the high density quantized state of EHL, and Auger recombination at the high density[30] plays an important role for shortening of the decay time.

Finally, some other things are discussed as follows. The emission peak of the recombination of EHL is determined by two factors, one is confinement effects of QD causing blueshift, another is many-body effects among electrons and holes in QD resulting in the redshift.[15,31–33] Because the intensity of laser beam has a Gauss distribution, carrier density at the center of the beam is much higher than that in outer. As EHL forming at the center of beam, the recombination of exciton still can be observed in the outer of beam. Therefore the emission of the exciton recombination is always in company with the emission of EHL. Similarly, the EHL will coexist with the electron-hole plasma, because critical excitation density always exists in Gauss distribution laser beam. The integrated intensity exhibiting a superlinear behavior as a function of the pump excitation density is attribute to a change of the oscillator strength of the radiative transitions as more carriers are added in the dots and their surrounding. This enhanced oscillator strength could result from a better overlap of electron and hole wave functions because of additional band bending effects.

IV. CONCLUSIONS

In summary, by using ps time-resolved PL, in a six-layer vertically coupled $In_{0.65}Al_{0.35}As/Al_{0.4}Ga_{0.6}As$ quantum dot array and at the sample temperature of 77 K, Fermi statistics of exciton state in the *s* and *p* shells of QD arrays is also observed at a sample temperature of 77 K. The observation of state-filling effect is due to the spectral linewidth shrinkage in an ensemble of QD array. The quantum dots are vertically aligned, leading to vertical coupling between exciton states in *s* and *p* shells from the different QDs. The time resolved photoluminescence reveals that the decay time of exciton states in the *p* shell is longer than that of the exciton state in the *s* shell of QD array. On the other hand, the spectral characteristics of EHL in QD array are demonstrated. After the formation of EHL and when the excitation density is not less than 365 W/cm^2, the recombination of the low-energy state from EHL is observed at 1.56 eV. While the excitation density is higher than 737 W/cm^2, the recombination of the high-energy state from EHL is also demonstrated at 1.59 eV. The spectral shape of the recombination of each quantum state shows independence on the excitation density within a certain range. The fact is attributed to the quantum confinement effect of QD. The lower peak energy shows a redshift of 200 meV away from that of the recombination of exciton states in the *s* and *p* shells. The transient spectral profile of the recombination of EHL keeps unchanging. However, after the long decay the central frequency shifts to the low. At the excitation density of 355 W/cm^2, the lifetime of electron-hole liquid is about 360 ps, while the decay time at the high excitation density decrease significantly.

ACKNOWLEDGMENTS

This work was supported by the National Natural Science Foundation of China (Grant No. 19934002 and 10274108), 973 (2003CB314901), 863 (2003AA311022) of China, and Natural Science Foundation of Guangdong Province of China.

*Corresponding author. Electronic address: stswhz@zsu.edu.cn

[1] A. Wójs, P. Hawrylak, S. Fafard, and L. Jacak, Physica E (Amsterdam) **2**, 603 (1998).
[2] S. Fafard, Z. R. Wasilewski, C. Ni. Allen, D. Picard, M. Spanner, J. P. McCaffrey, and P. G. Piva, Phys. Rev. B **59**, 15 368 (1999).
[3] M. Bayer, O. Stern, P. Hawrylak, S. Fafrad, and A. Forchel, Nature (London) **405**, 923 (2000).
[4] U. Bockelmann, Ph. Roussignol, A. Filoramo, W. Heller, G. Abstreiter, K. Brunner, G. Böhm, and G. Weimann, Phys. Rev. Lett. **76**, 3622 (1996).
[5] K. Hinzer, P. Hawrylak, M. Korkusinski, S. Fafard, M. Bayer, O. Stern, A. Gorbunov, and A. Forchel, Phys. Rev. B **63**, 075314 (2001).
[6] *Electron-Hole Droplets in Semiconductors*, edited by C. D. Jeffries and L. V. Keldysh (North-Holland, Amsterdam, 1983).
[7] L. M. Smith and J. P. Wolfe, Phys. Rev. B **51**, 7521 (1995).
[8] J. Shah and R. F. Leheny, W. R. Harding, and D. R. Wight, Phys. Rev. Lett. **38**, 1164 (1977).
[9] H. Kalt, K. Reimann, W. W. Rühle, M. Rinker, and E. Bauser, Phys. Rev. B **42**, 7058 (1990).
[10] D. Bimberg, M. S. Skolnick, and W. J. Choyke, Phys. Rev. Lett. **40**, 56 (1978).
[11] R. Shimano, M. Nagai, K. Horiuch, and M. Kuwata-Gonokami, Phys. Rev. Lett. **88**, 057404 (2002); M. Nagai, R. Shimano, K. Horiuch, and M. Kuwata-Gonokami, Phys. Rev. B **68**, 081202(R) (2003); M. A. Vouk, J. Phys. C **12**, 2305 (1979).
[12] M. Nagai, R. Shimano, and M. Kuwata-Gonokami, Phys. Rev. Lett. **86**, 5795 (2001); M. Nagai and M. Kuwata-Gonokami, J. Lumin. **100**, 233 (2002).
[13] R. F. Leheny and J. Shah, Phys. Rev. Lett. **38**, 511 (1977).

[14] H. Y. Liu, I. R. Sellers, R. J. Airey, M. J. Steer, P. A. Houston D. J. Mowbray, J. Cockburn, M. S. Skolnick, B. Xu, and Z. G. Wang, Appl. Phys. Lett. **80**, 3769 (2002).
[15] A. J. Williamson, A. Franceschetti, and A. Zunger, Europhys. Lett. **53**, 59 (2001).
[16] A. Wójs, P. Hawrylak, and J. J. Quinn, Phys. Rev. B **60**, 11 661 (1999).
[17] N. Perret, D. Morris, L. Franchomme-Fossé, R. Côté, S. Fafard, V. Aimez, and J. Beauvais, Phys. Rev. B **62**, 5092 (2000).
[18] T. Mano, R. NÖtzel, G. J. Hamhuis, T. J. Eijkemans, and J. H. Wolter, Appl. Phys. Lett. **81**, 1705 (2002).
[19] J. W. Tomm, T. Elsaesser, Y. I. Mazur, H. Kissel, G. G. Tarasov, Z. Ya. Zhuchenko, and W. T. Masselink, Phys. Rev. B **67**, 045326 (2003).
[20] R. Leon, J. Ibàñez, S. Marcinkevičius, J. Siegert, T. Paskova, B. Monemar, S. Chaparro, C. Navarro, S. R. Johnson, and Y.-H. Zhang, Phys. Rev. B **66**, 085331 (2002).
[21] K. Hinzer, S. Fafard, A. J. SpringThorpe, J. Arlett, E. M. Griswold, Y. Feng, and S. Charbonneau, Physica E (Amsterdam) **2**, 729 (1998).
[22] P. Borri, W. Langbein, S. Schneider, U. Woggon, R. L. Sellin, D. Ouyang, and D. Bimberg, Phys. Rev. Lett. **87**, 157401 (2001).
[23] A. V. Filinov, M. Bonitz, and Y. E. Lozovik, J. Phys. A **36**, 5899 (2003).
[24] P. D. Wang, J. L. Merz, S. Fafard, R. Leon, D. Leonard, G. Medeiros-Ribeiro, M. Oestreich, P. M. Petroff, K. Uchida, N. Miura, H. Akiyama, and H. Sakaki, Phys. Rev. B **53**, 16 458 (1996).
[25] S. Schmitt-Rink, D. A. B. Miller, and D. S. Chemla, Phys. Rev. B **35**, 8113 (1987); S. Öğüt, J. R. Chelikowsky, and S. G. Louie, Phys. Rev. Lett. **79**, 1770 (1997).
[26] R. Tsu, Appl. Phys. A: Mater. Sci. Process. **71**, 391 (2000); L. V. Keldysh, Phys. Status Solidi A **164**, 3 (1997).
[27] V. Ranjan and V. A. Singh, J. Appl. Phys. **89**, 6415 (2001).
[28] L. W. Wang and A. Zunger, Phys. Rev. Lett. **73**, 1039 (1994).
[29] T. Koga, J. Nitta, H. Takayanagi, and S. Datta, Phys. Rev. Lett. **88**, 126601 (2002).
[30] U. Bockelmann and T. Egeler, Phys. Rev. B **46**, 15 574 (1992).
[31] R. Heitz, F. Guffarth, I. Mukhametzhanov, M. Grundmann, A. Madhukar, and D. Bimberg, Phys. Rev. B **62**, 16 881 (2000).
[32] A. Orlandi, M. Rontani, G. Goldoni, F. Manghi, and E. Molinari Phys. Rev. B **63**, 045310 (2001).
[33] D. A. Kleinman, Phys. Rev. B **33**, 2540 (1985).